Experimental data analysis techniques for validation of tokamak impurity transport simulations

M.A. Chilenski

MIT Department of Nuclear Science and Engineering

October 13, 2016

This material is based upon work conducted using the Alcator C-Mod tokamak, a DOE Office of Science user facility. This material is based upon work supported by the U.S. Department of Energy, Office of Science, Office of Fusion Energy Sciences under Award Number DE-FC02-99ER54512. This material is based upon work supported in part by the U.S. Department of Energy Office of Science Graduate Research Fellowship Program (DOE SCGF), made possible in part by the American Recovery and Reinvestment Act of 2009, administered by ORISE-ORAU under contract number DE-AC05-06OR23100. The XEUS and LoWEUS spectrometers were developed at the LLNL EBIT lab. Work at LLNL was performed under the auspices of the US DOE under contract DE-AC52-07NA-27344. Some of the computations using STRAHL were carried out on the MIT PSFC parallel AMD Opteron/Infiniband cluster Loki.

Experimental data analysis techniques for validation of tokamak impurity transport simulations

1. Motivation: validation of turbulent transport simulations
2. Profile fitting with nonstationary Gaussian process regression
3. Inferring impurity transport coefficients: a very difficult inverse problem
4. Conclusions and future directions

Experimental data analysis techniques for validation of tokamak impurity transport simulations

1. Motivation: validation of turbulent transport simulations
2. Profile fitting with nonstationary Gaussian process regression
3. Inferring impurity transport coefficients: a very difficult inverse problem
4. Conclusions and future directions

Motivation: nuclear fusion and impurity transport

Ideal situation

- Make plasma, heat it up.
- Energy is produced faster than it is lost.
- Impurities do not accumulate.
- Clean, sustainable energy for everyone!

What actually happens

- Make plasma, heat it up.
- Turbulence causes energy to leak out.
- Impurities accumulate, further contributing to energy loss.
- No net energy gain.

Options

- Build bigger and bigger tokamaks until we finally get one big enough to hold its energy in. $$$ =
- Develop predictive simulations, figure out how to optimize the configuration *before* building an expensive facility. $$ =

Motivation: validation of impurity transport simulations

Options

- Build bigger and bigger tokamaks until we finally get one big enough to hold its energy in. $\$\$\$ =$ ☹
- **Develop predictive simulations, figure out how to optimize the configuration *before* building an expensive facility.** $\$\$ =$ ☺

How do we get there?

- Need to test simulations against existing experiments.
- Highly sensitive to gradients: *all* validation work benefits from improved gradient measurements.
- Impurity transport measurements are key:
  - Of fundamental importance to setting the power balance.
  - Another channel to check turbulent transport simulations with.

Experimental data analysis techniques for validation of tokamak impurity transport simulations

Profile fitting: a critical step for plasma data analysis

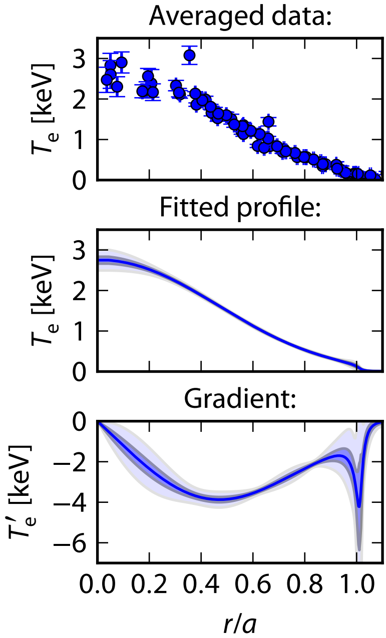

- Transport codes are highly sensitive to *gradients* in n_e, T_e, etc.
- Many codes require *entire profiles* as inputs.
- Need to propagate profile uncertainties efficiently.

Gaussian process regression (GPR) overcomes the many issues with previous approaches to profile fitting

Old: Splines

- Fit data with piecewise polynomial.
- Software readily available.
- Pick properties by eye: subjective, time consuming.
- Inefficient propagation of profile uncertainty.

New: GPR

- Fit data with multivariate normal distribution.
- New software had to be written.
- Pick properties with statistically rigorous, automated procedure.
- Enables efficient uncertainty propagation.

Gaussian process regression (GPR): a statistically rigorous method to fit profiles, propagate uncertainty

- Describe data y, fit y_* as a multivariate normal distribution.
- Can include derivatives, line integrals.

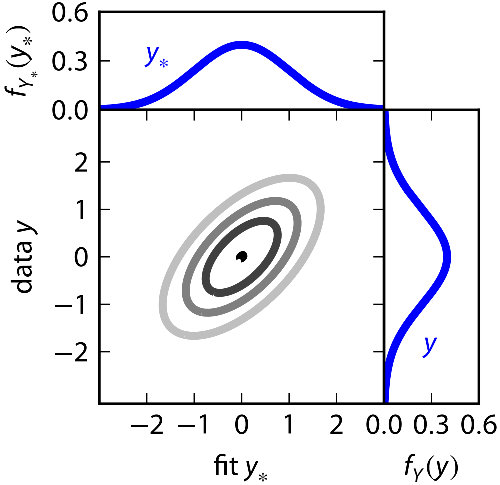

Gaussian process regression (GPR): a statistically rigorous method to fit profiles, propagate uncertainty

- Describe data y, fit y_* as a multivariate normal distribution.
- Can include derivatives, line integrals.

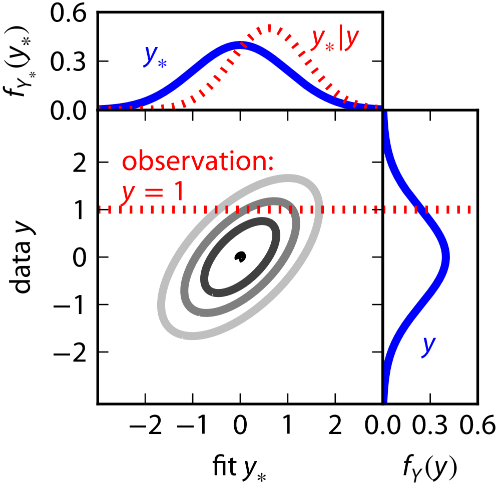

The covariance kernel sets the smoothness

Covariance kernel

$k(x_1, x_2) = \mathrm{cov}[y_1, y_2]$ sets how spatial covariance decays:

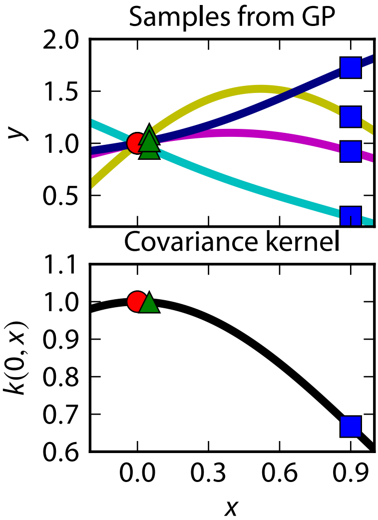

Key step: infer hyperparameters $\boldsymbol{\theta}$ of covariance kernel:

- maximize $f_{\boldsymbol{\Theta}|\boldsymbol{Y}}(\boldsymbol{\theta}|\boldsymbol{y})$, or
- sample $\widetilde{\boldsymbol{\theta}} \sim f_{\boldsymbol{\Theta}|\boldsymbol{Y}}(\boldsymbol{\theta}|\boldsymbol{y})$

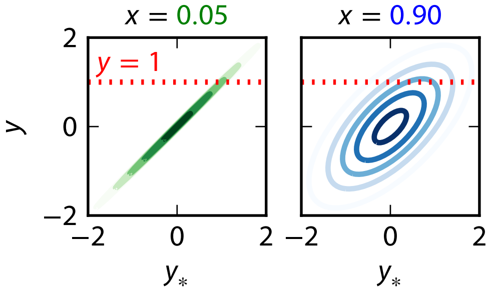

Demonstration: L-mode temperature profile

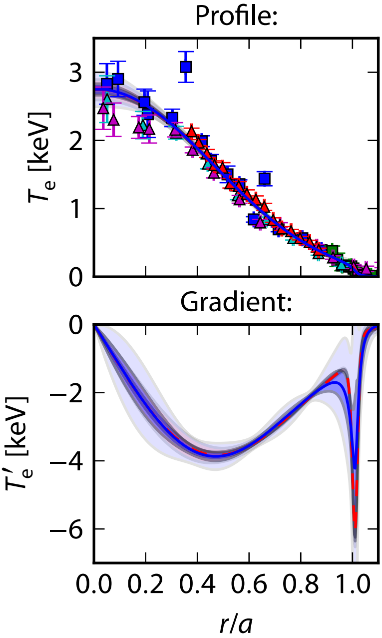

- Combine data from core TS, edge TS, GPC, GPC2, FRCECE
- Force $\mathrm{d}T_e/\mathrm{d}r = 0$ at $r = 0$
- Handling the hyperparameters $\boldsymbol{\theta}$:
  - MAP: $\hat{\boldsymbol{\theta}} = \arg\max_{\boldsymbol{\theta}} f_{\boldsymbol{\Theta}|\boldsymbol{Y}}(\boldsymbol{\theta}|\boldsymbol{y})$
  - MCMC: $f_{\boldsymbol{Y}_*|\boldsymbol{Y}}(\boldsymbol{y}_*|\boldsymbol{y}) = \int f_{\boldsymbol{Y}_*|\boldsymbol{Y},\boldsymbol{\Theta}}(\boldsymbol{y}_*|\boldsymbol{y},\boldsymbol{\theta}) f_{\boldsymbol{\Theta}|\boldsymbol{Y}}(\boldsymbol{\theta}|\boldsymbol{y})\,\mathrm{d}\boldsymbol{\theta}$
- **Key result:** $\sigma_{T_{e,\mathrm{MCMC}}} \approx \sigma_{T_{e,\mathrm{MAP}}}$, $\sigma_{a/L_{T_{e,\mathrm{MCMC}}}} \approx 2.6 \times \sigma_{a/L_{T_{e,\mathrm{MAP}}}}$
- Can use fast MAP when only value matters 🙂, but need slow MCMC when gradients matter ☹
- Software: gptools.readthedocs.io

GPR can help with all validation activities.

Demonstration: L-mode temperature profile

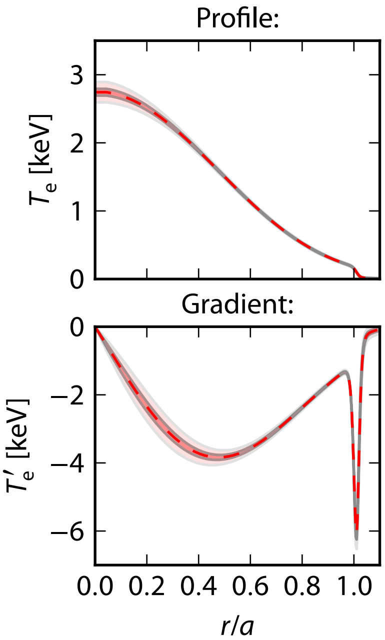

- Combine data from core TS, edge TS, GPC, GPC2, FRCECE
- Force $\mathrm{d}T_\mathrm{e}/\mathrm{d}r = 0$ at $r = 0$
- Handling the hyperparameters $\boldsymbol{\theta}$:
  - MAP: $\hat{\boldsymbol{\theta}} = \arg\max_{\boldsymbol{\theta}} f_{\boldsymbol{\Theta}|\boldsymbol{Y}}(\boldsymbol{\theta}|\boldsymbol{y})$
  - MCMC: $f_{\boldsymbol{Y}_*|\boldsymbol{Y}}(\boldsymbol{y}_*|\boldsymbol{y}) = \int f_{\boldsymbol{Y}_*|\boldsymbol{Y},\boldsymbol{\Theta}}(\boldsymbol{y}_*|\boldsymbol{y},\boldsymbol{\theta}) f_{\boldsymbol{\Theta}|\boldsymbol{Y}}(\boldsymbol{\theta}|\boldsymbol{y})\,\mathrm{d}\boldsymbol{\theta}$
- **Key result:** $\sigma_{T_{\mathrm{e,MCMC}}} \approx \sigma_{T_{\mathrm{e,MAP}}}$, $\sigma_{a/L_{T_{\mathrm{e,MCMC}}}} \approx 2.6 \times \sigma_{a/L_{T_{\mathrm{e,MAP}}}}$
- Can use fast MAP when only value matters 🙂, but need slow MCMC when gradients matter 🙁
- Software: gptools.readthedocs.io

GPR can help with all validation activities.

Demonstration: L-mode temperature profile

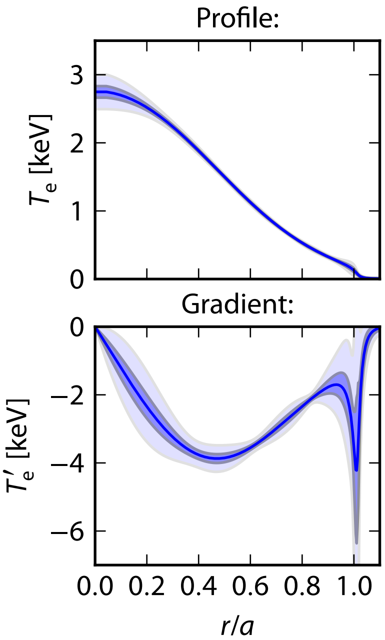

- Combine data from core TS, edge TS, GPC, GPC2, FRCECE
- Force $\mathrm{d}T_e/\mathrm{d}r = 0$ at $r = 0$
- Handling the hyperparameters $\boldsymbol{\theta}$:
  - MAP: $\hat{\boldsymbol{\theta}} = \arg\max_{\boldsymbol{\theta}} f_{\boldsymbol{\Theta}|\boldsymbol{Y}}(\boldsymbol{\theta}|\boldsymbol{y})$
  - MCMC: $f_{\boldsymbol{Y}_*|\boldsymbol{Y}}(\boldsymbol{y}_*|\boldsymbol{y}) = \int f_{\boldsymbol{Y}_*|\boldsymbol{Y},\boldsymbol{\Theta}}(\boldsymbol{y}_*|\boldsymbol{y},\boldsymbol{\theta}) f_{\boldsymbol{\Theta}|\boldsymbol{Y}}(\boldsymbol{\theta}|\boldsymbol{y})\,\mathrm{d}\boldsymbol{\theta}$
- **Key result:** $\sigma_{T_{e,\mathrm{MCMC}}} \approx \sigma_{T_{e,\mathrm{MAP}}}$, $\sigma_{a/L_{T_{e,\mathrm{MCMC}}}} \approx 2.6 \times \sigma_{a/L_{T_{e,\mathrm{MAP}}}}$
- Can use fast MAP when only value matters, but need slow MCMC when gradients matter
- Software: gptools.readthedocs.io

GPR can help with all validation activities.

Demonstration: L-mode temperature profile

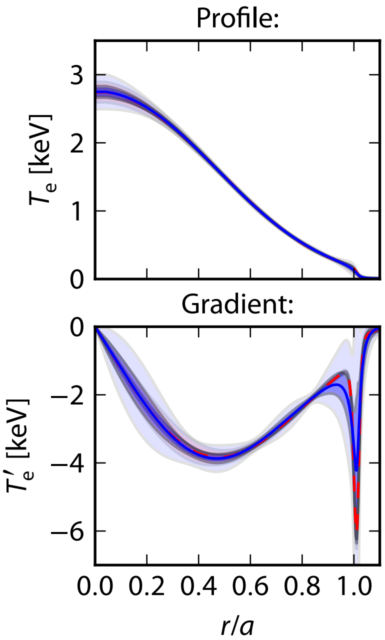

- Combine data from core TS, edge TS, GPC, GPC2, FRCECE
- Force $\mathrm{d}T_\mathrm{e}/\mathrm{d}r = 0$ at $r = 0$
- Handling the hyperparameters $\boldsymbol{\theta}$:
  - MAP: $\hat{\boldsymbol{\theta}} = \arg\max_{\boldsymbol{\theta}} f_{\boldsymbol{\Theta}|\boldsymbol{Y}}(\boldsymbol{\theta}|\boldsymbol{y})$
  - MCMC: $f_{\boldsymbol{Y}_*|\boldsymbol{Y}}(\boldsymbol{y}_*|\boldsymbol{y}) = \int f_{\boldsymbol{Y}_*|\boldsymbol{Y},\boldsymbol{\Theta}}(\boldsymbol{y}_*|\boldsymbol{y},\boldsymbol{\theta}) f_{\boldsymbol{\Theta}|\boldsymbol{Y}}(\boldsymbol{\theta}|\boldsymbol{y})\,\mathrm{d}\boldsymbol{\theta}$
- **Key result:** $\sigma_{T_{\mathrm{e,MCMC}}} \approx \sigma_{T_{\mathrm{e,MAP}}}$, $\sigma_{a/L_{T_{\mathrm{e,MCMC}}}} \approx 2.6 \times \sigma_{a/L_{T_{\mathrm{e,MAP}}}}$
- Can use fast MAP when only value matters, but need slow MCMC when gradients matter
- Software: gptools.readthedocs.io

GPR can help with all validation activities.

Demonstration: L-mode temperature profile

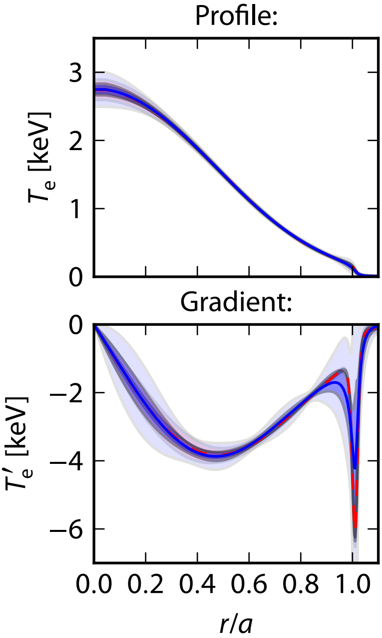

- Combine data from core TS, edge TS, GPC, GPC2, FRCECE
- Force $\mathrm{d}T_e/\mathrm{d}r = 0$ at $r = 0$
- Handling the hyperparameters $\boldsymbol{\theta}$:
  - MAP: $\hat{\boldsymbol{\theta}} = \arg\max_{\boldsymbol{\theta}} f_{\boldsymbol{\Theta}|\boldsymbol{Y}}(\boldsymbol{\theta}|\boldsymbol{y})$
  - MCMC: $f_{\boldsymbol{Y}_*|\boldsymbol{Y}}(\boldsymbol{y}_*|\boldsymbol{y}) = \int f_{\boldsymbol{Y}_*|\boldsymbol{Y},\boldsymbol{\Theta}}(\boldsymbol{y}_*|\boldsymbol{y},\boldsymbol{\theta}) f_{\boldsymbol{\Theta}|\boldsymbol{Y}}(\boldsymbol{\theta}|\boldsymbol{y})\,\mathrm{d}\boldsymbol{\theta}$
- **Key result:** $\sigma_{T_{e,\mathrm{MCMC}}} \approx \sigma_{T_{e,\mathrm{MAP}}}$, $\sigma_{a/L_{T_{e,\mathrm{MCMC}}}} \approx 2.6 \times \sigma_{a/L_{T_{e,\mathrm{MAP}}}}$
- Can use fast MAP when only value matters, but need slow MCMC when gradients matter
- Software: gptools.readthedocs.io

GPR can help with all validation activities.

Experimental data analysis techniques for validation of tokamak impurity transport simulations

Inferring impurity transport coefficients: a nonlinear inverse problem

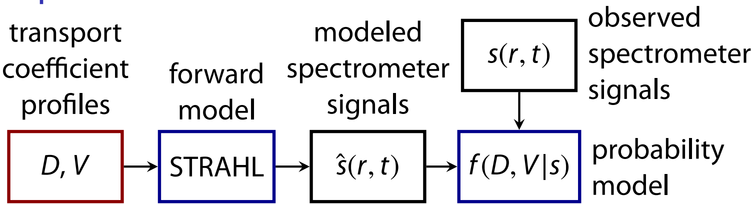

- Diffusion coefficient D, convective velocity V.
- Can only observe s, want to know D, V.
- Only know the forward mapping: $\hat{s} = m(D, V)$, but want $D, V = m^{-1}(s)$.
- Key questions:

Existence:	Is there a D, V such that $\hat{s} \approx s$?
Uniqueness:	How many D, V are there such that $\hat{s} \approx s$?
Stability:	How much do D, V change when I perturb s?

What is wrong, and what I have done about it

Previous methods have substantial shortcomings

- Error bars not consistent with intuition.
- Cannot handle sawteeth.
- Different starting points give different results:
  - Multiple solutions?
  - Broad region of acceptable solutions?

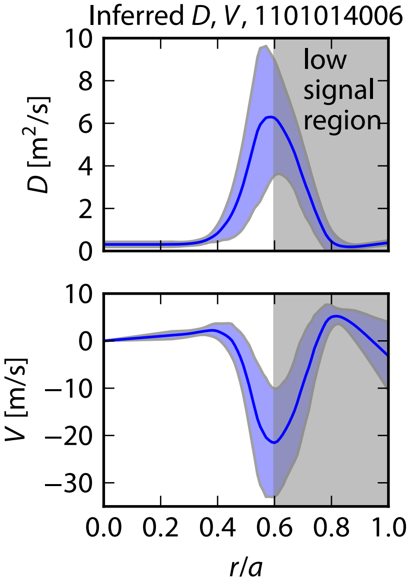

What is wrong, and what I have done about it

Previous methods have substantial shortcomings

- Error bars not consistent with intuition.
- Cannot handle sawteeth.
- Different starting points give different results:
  - Multiple solutions?
  - Broad region of acceptable solutions?

Attack the problem two ways

- **Fast, linearized model** to get order-of-magnitude
- **Slow, complete procedure**

Surprising results

- Spatial resolution trumps temporal resolution.
- n_e, T_e do not matter.
- Selecting the appropriate complexity for D, V is really, really important.

Painfully simple transport coefficient profiles produce behaviors representative of what is seen experimentally

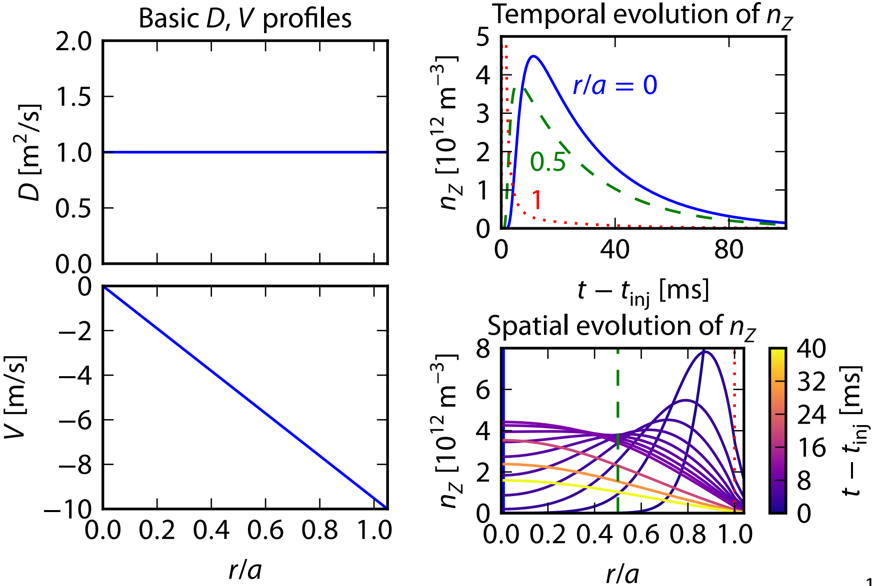

Three figures of merit capture most of the information

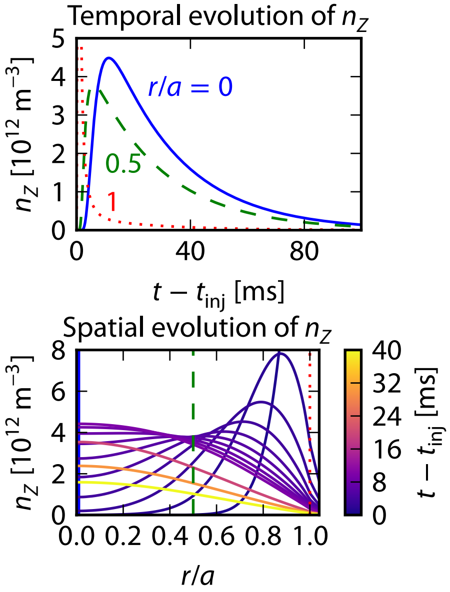

- Informed by theoretical analysis in [Seguin PRL 1983] and [Fussmann NF 1986].
- **Impurity confinement time:** $\tau_{imp} \sim f(V/D)/D$
- **Rise time** (of core): $t_r \sim f(D)$
- **Profile broadness** (during decay): $b_{r/a} = n_Z(r/a)/n_Z(0) \sim f(V/D)$

τ_{imp}, t_{r}, $b_{0.75}$ are all different functions of D, V

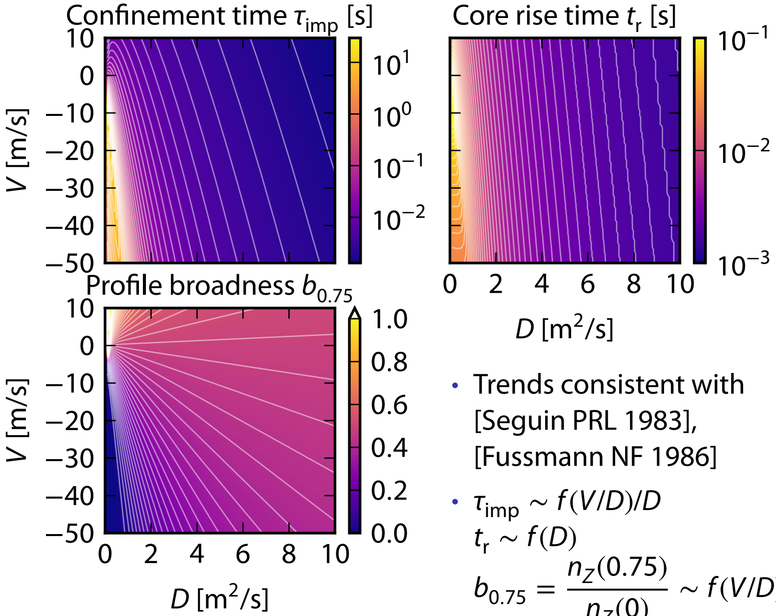

- Trends consistent with [Seguin PRL 1983], [Fussmann NF 1986]
- $\tau_{\mathrm{imp}} \sim f(V/D)/D$
  $t_{\mathrm{r}} \sim f(D)$
  $b_{0.75} = \dfrac{n_Z(0.75)}{n_Z(0)} \sim f(V/D)$

The unique intersection of the contours of τ_{imp}, t_{r} and $b_{0.75}$ determines D, V

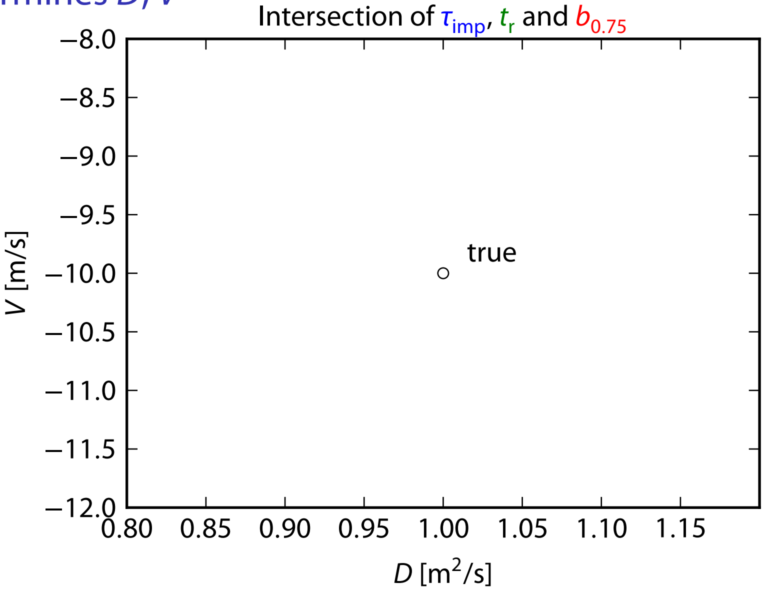

The unique intersection of the contours of τ_{imp}, t_{r} and $b_{0.75}$ determines D, V

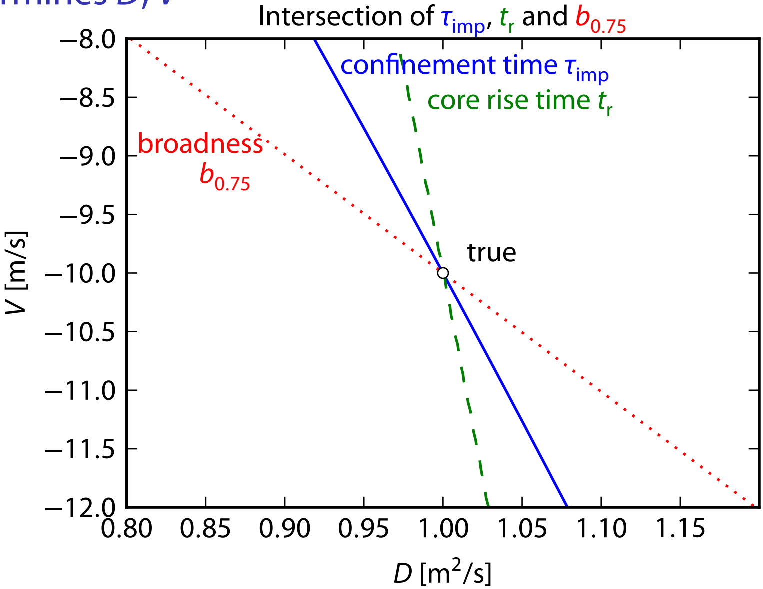

The unique intersection of the contours of τ_{imp}, t_r and $b_{0.75}$ determines D, V

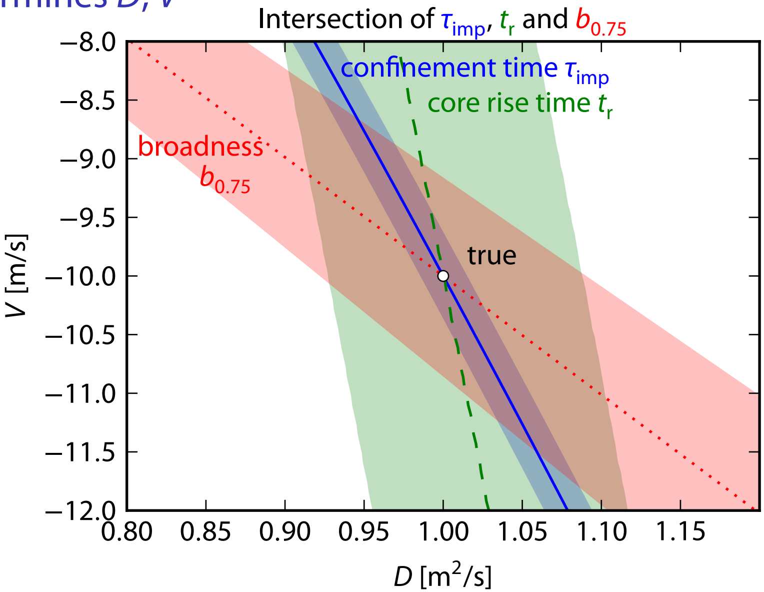

The unique intersection of the contours of τ_{imp}, t_r and $b_{0.75}$ determines D, V

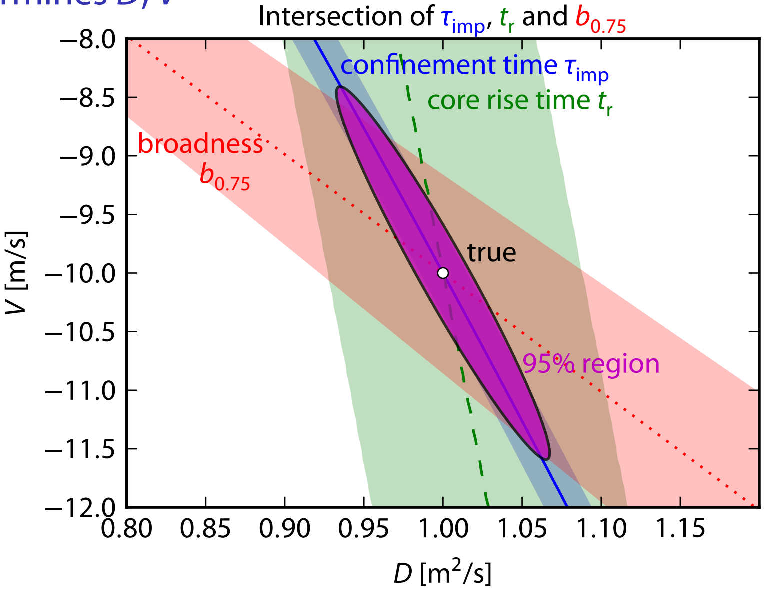

Making the picture quantitative

- Linearize each figure of merit $y_i = g_i(D, V)$ with respect to D, V.
- Assume Gaussian noise: $y_i \sim \mathcal{N}(\mu_{y_i}, \sigma_{y_i}^2)$.
- Transport coefficient vector $\boldsymbol{T} = [D, V]^\mathsf{T} \sim \mathcal{N}(\boldsymbol{\mu}_{\boldsymbol{T}|\boldsymbol{y}}, \boldsymbol{\Sigma}_{\boldsymbol{T}|\boldsymbol{y}})$:

$$\boldsymbol{\mu}_{\boldsymbol{T}|\boldsymbol{y}} = (\mathbf{C}^\mathsf{T}\boldsymbol{\Sigma}_{\boldsymbol{y}}^{-1}\mathbf{C})^{-1}\left(\mathbf{C}^\mathsf{T}\boldsymbol{\Sigma}_{\boldsymbol{y}}^{-1}(\boldsymbol{y} - \boldsymbol{a})\right)$$
$$\boldsymbol{\Sigma}_{\boldsymbol{T}|\boldsymbol{y}} = (\mathbf{C}^\mathsf{T}\boldsymbol{\Sigma}_{\boldsymbol{y}}^{-1}\mathbf{C})^{-1}$$

- $\boldsymbol{\mu}_{\boldsymbol{T}|\boldsymbol{y}}$ is the actual prediction of $\boldsymbol{T} = [D, V]^\mathsf{T}$,
  $\boldsymbol{\Sigma}_{\boldsymbol{T}|\boldsymbol{y}}$ contains the uncertainties.
- $\boldsymbol{a}$ and $\mathbf{C}$ come from the linearization.
- $\boldsymbol{y}$ contains the actual observations,
  $\boldsymbol{\Sigma}_{\boldsymbol{y}}$ contains the uncertainties.

This is exactly the result of *weighted least squares regression:* the analysis attempts to match the observations in the least squares sense.

The linearized model can estimate the uncertainties on D and V given the uncertainties on τ_{imp}, t_{r} and $b_{0.75}$

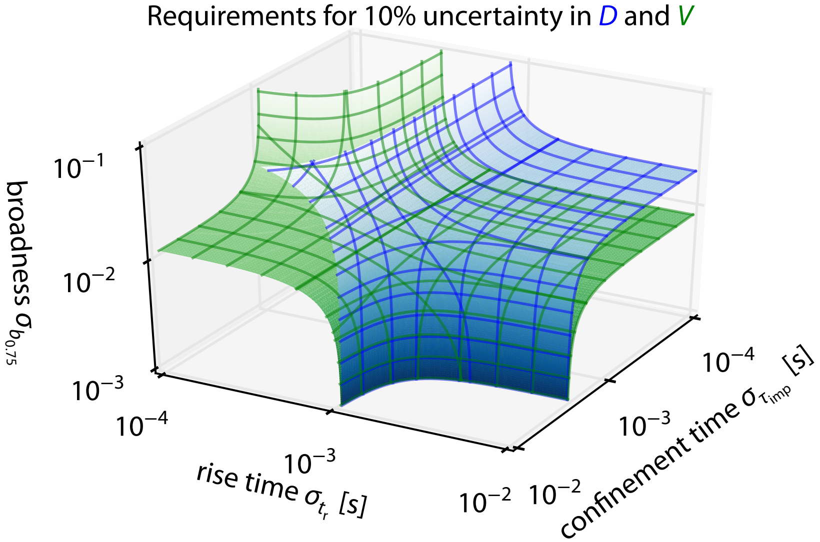

Either rise time or broadness needs to be known to high precision

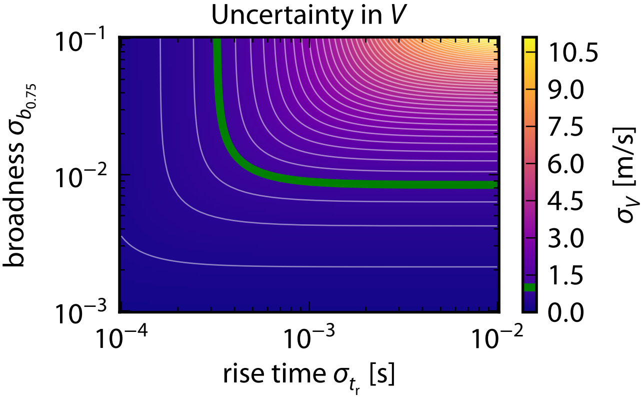

- Green contour: $\sigma_V/V_0 = \pm 10\%$ (what previous plot gave).
- Assume confinement time is known precisely.
- **Only need to know *one* of t_r or $b_{0.75}$ to high precision:** only a limited window where they are on an equal footing.

Characterizing the diagnostic requirements

Three key parameters:

1. Number of channels, N
2. The time resolution, Δt
3. The relative noise level, $u = \sigma_s/s$

Method:

1. Generate many synthetic data sets with different realizations of Gaussian noise and phase with respect to injection.
2. Determine τ_{imp}, t_{r} and $b_{r/a} = n_Z(r/a)/n_Z(0)$ for each realization.
3. Compute $\sigma_{\tau_{\mathrm{imp}}}$, $\sigma_{t_{\mathrm{r}}}$ and $\sigma_{b_{r/a}}$ from the ensemble of fits.
4. Compute σ_D and σ_V.

Spatial resolution is more important than time resolution

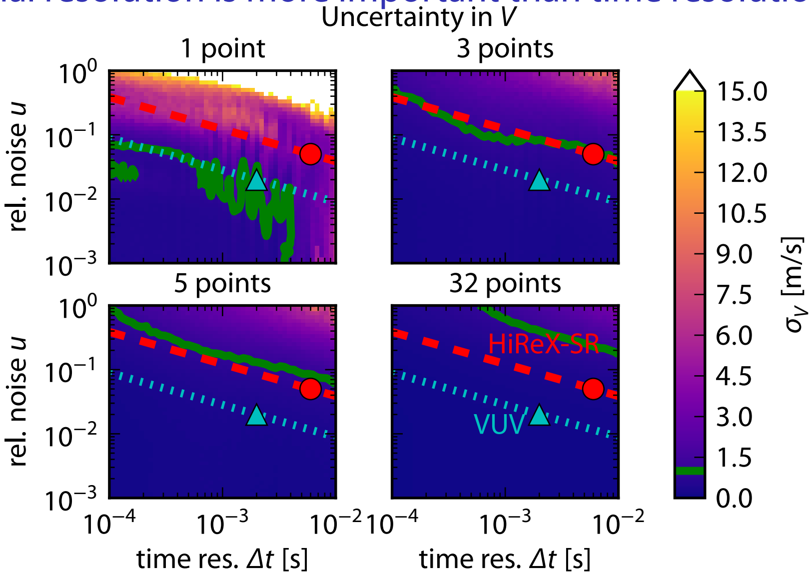

Dashed lines: contours of constant photon rate

Green contours: $\sigma_V/V_0 = \pm 10\%$

Implications of the linearized model

- C-Mod's diagnostics appear to be sufficient to reproduce simple D, V profiles.
- Spatial resolution is more important than time resolution:
  - Better to invest in *more* detectors than *fancier* detectors.
  - Can handle sawteeth by using a *single* injection.

Caveats

- Ignored details of tomographic inversion.
- Threw out lots of other information in the signals.
- Used painfully oversimplified D, V profiles.

Building the full analysis: two key steps to inference

Bayes' rule combines information from data with prior knowledge/constraints:

$$\underbrace{f_{D,V|y}(D,V|y)}_{\substack{\text{posterior:}\\ \text{everything known about } D,\, V}} = \frac{\overbrace{f_{y|D,V}(y|D,V)}^{\substack{\text{likelihood:}\\ \text{information from data } y}} \cdot \overbrace{f_{D,V}(D,V)}^{\substack{\text{prior:}\\ \text{prior knowledge, constraints}}}}{\underbrace{f_y(y)}_{\substack{\text{evidence:}\\ \text{probability of data}\\ \text{under given parameterization, } \mathcal{M}}}}$$

Parameter estimation Find the values of D, V consistent with the data y: characterize $f_{D,V|y}(D,V|y)$.

Model selection Find the best way of parameterizing D, V by maximizing $f_y(y)$.

MultiNest [Feroz MNRAS 2008, 2009; Buchner AA 2014] produces samples from $f_{D,V|y}(D,V|y)$ *and* an estimate of $f_y(y)$.
Can handle multimodal posterior distributions.

Building the full analysis: two key steps to inference

Bayes' rule combines information from data with prior knowledge/constraints:

$$\underbrace{f_{D,V|y}(D,V|y)}_{\substack{\text{posterior:}\\ \text{everything known about } D,\,V}} = \frac{\overbrace{f_{y|D,V}(y|D,V)}^{\substack{\text{likelihood:}\\ \text{information from data } y}} \cdot \overbrace{f_{D,V}(D,V)}^{\substack{\text{prior:}\\ \text{prior knowledge, constraints}}}}{\underbrace{f_y(y)}_{\substack{\text{evidence:}\\ \text{probability of data}\\ \textit{under given parameterization, } \mathcal{M}}}}$$

Parameter estimation Find the values of D, V consistent with the data y: characterize $f_{D,V|y}(D,V|y)$.

Model selection Find the best way of parameterizing D, V by maximizing $f_y(y)$.

MultiNest [Feroz MNRAS 2008, 2009; Buchner AA 2014] produces samples from $f_{D,V|y}(D,V|y)$ *and* an estimate of $f_y(y)$.
Can handle multimodal posterior distributions.

Building the full analysis: two key steps to inference

Bayes' rule combines information from data with prior knowledge/constraints:

$$\underbrace{f_{D,V|y}(D,V|y)}_{\substack{\text{posterior:}\\ \text{everything known about } D,\,V}} = \frac{\overbrace{f_{y|D,V}(y|D,V)}^{\substack{\text{likelihood:}\\ \text{information from data } y}} \cdot \overbrace{f_{D,V}(D,V)}^{\substack{\text{prior:}\\ \text{prior knowledge, constraints}}}}{\underbrace{f_y(y)}_{\substack{\text{evidence:}\\ \text{probability of data}\\ \textit{under given parameterization, } \mathcal{M}}}}$$

Parameter estimation — Find the values of D, V consistent with the data y: characterize $f_{D,V|y}(D,V|y)$.

Model selection — Find the best way of parameterizing D, V by maximizing $f_y(y)$.

MultiNest [Feroz MNRAS 2008, 2009; Buchner AA 2014] produces samples from $f_{D,V|y}(D,V|y)$ *and* an estimate of $f_y(y)$.
Can handle multimodal posterior distributions.

Building the full analysis: two key steps to inference

Bayes' rule combines information from data with prior knowledge/constraints:

$$\underbrace{f_{D,V|y,\mathcal{M}}(D,V|y,\mathcal{M})}_{\substack{\text{posterior:}\\ \text{everything known about } D,\,V}} = \frac{\overbrace{f_{y|D,V,\mathcal{M}}(y|D,V,\mathcal{M})}^{\substack{\text{likelihood:}\\ \text{information from data } y}} \cdot \overbrace{f_{D,V|\mathcal{M}}(D,V|\mathcal{M})}^{\substack{\text{prior:}\\ \text{prior knowledge, constraints}}}}{\underbrace{f_{y|\mathcal{M}}(y|\mathcal{M})}_{\substack{\text{evidence:}\\ \text{probability of data}\\ \textit{under given parameterization, } \mathcal{M}}}}$$

Parameter estimation: Find the values of D, V consistent with the data y: characterize $f_{D,V|y,\mathcal{M}}(D,V|y,\mathcal{M})$.

Model selection: Find the best way of parameterizing D, V by maximizing $f_{y|\mathcal{M}}(y|\mathcal{M})$.

MultiNest [Feroz MNRAS 2008, 2009; Buchner AA 2014] produces samples from $f_{D,V|y,\mathcal{M}}(D,V|y,\mathcal{M})$ *and* an estimate of $f_{y|\mathcal{M}}(y|\mathcal{M})$. Can handle multimodal posterior distributions.

Building the full analysis: two key steps to inference

Bayes' rule combines information from data with prior knowledge/constraints:

$$\underbrace{f_{D,V|y,\mathcal{M}}(D,V|y,\mathcal{M})}_{\substack{\text{posterior:}\\ \text{everything known about } D,\,V}} = \frac{\overbrace{f_{y|D,V,\mathcal{M}}(y|D,V,\mathcal{M})}^{\substack{\text{likelihood:}\\ \text{information from data } y}} \cdot \overbrace{f_{D,V|\mathcal{M}}(D,V|\mathcal{M})}^{\substack{\text{prior:}\\ \text{prior knowledge, constraints}}}}{\underbrace{f_{y|\mathcal{M}}(y|\mathcal{M})}_{\substack{\text{evidence:}\\ \text{probability of data}\\ \textit{under given parameterization, } \mathcal{M}}}}$$

Parameter estimation: Find the values of D, V consistent with the data y: characterize $f_{D,V|y,\mathcal{M}}(D,V|y,\mathcal{M})$.

Model selection: Find the best way of parameterizing D, V by maximizing $f_{y|\mathcal{M}}(y|\mathcal{M})$.

MultiNest [Feroz MNRAS 2008, 2009; Buchner AA 2014] produces samples from $f_{D,V|y,\mathcal{M}}(D,V|y,\mathcal{M})$ *and* an estimate of $f_{y|\mathcal{M}}(y|\mathcal{M})$. Can handle multimodal posterior distributions.

MultiNest successfully reconstructs simple *D*, *V* profiles

(synthetic data)

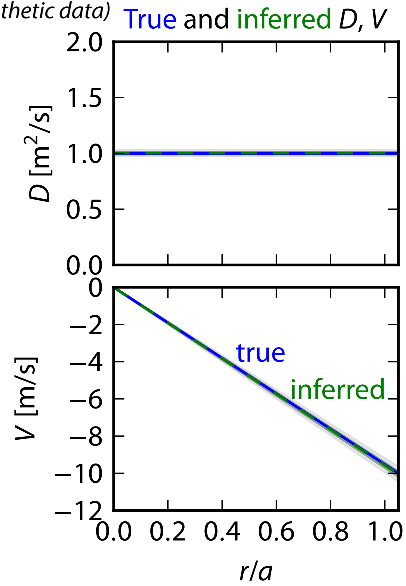

- Five local measurements
- $\Delta t = 6\,\mathrm{ms}$, 5% noise
- Have also tested with 32 HiReX-SR chords
- 5× smaller σ_D, σ_V than linearized analysis, *but same correlation*

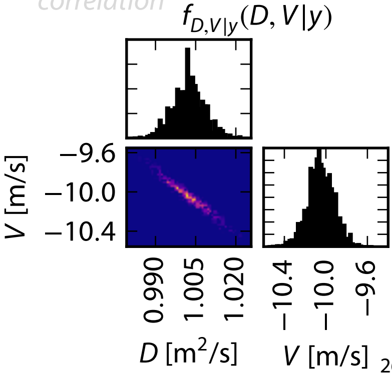

MultiNest successfully reconstructs simple D, V profiles

(synthetic data)

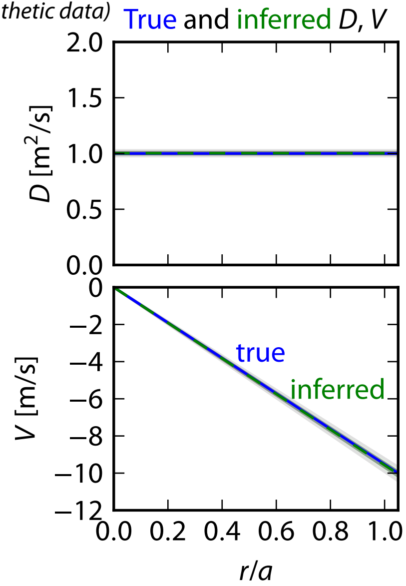

- Five local measurements
- $\Delta t = 6$ ms, 5% noise
- Have also tested with 32 HiReX-SR chords
- 5× smaller σ_D, σ_V than linearized analysis, *but same correlation*

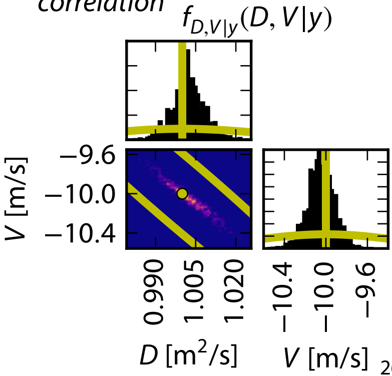

Previous analysis ascribed all uncertainty in D, V to n_e, T_e

(experimental data)

Previous approach [Howard NF 2012, Chilenski NF 2015]:

1. Model D, V with piecewise linear splines.
2. Generate random samples of n_e, T_e according to diagnostic uncertainties.
3. For each n_e, T_e realization, generate a random distribution of spline knots.
4. Given n_e, T_e and the spline knots, run an optimizer to find the best-fitting D, V profiles.
5. Find mean, standard deviation of resulting profiles.

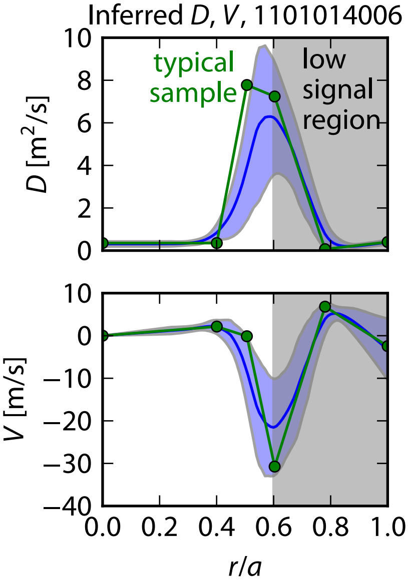

New result: n_e, T_e have little effect on D, V

(synthetic data)

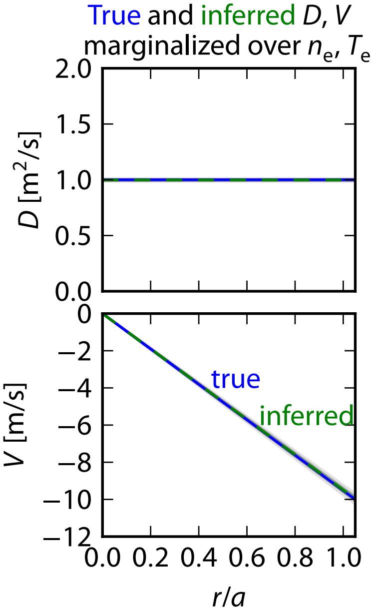

- 32 HiReX-SR chords, $\Delta t = 6$ ms, 5% noise
- Fit n_e, T_e with GPR, propagated uncertainty using 3 eigenvalues for each.
- **Result is identical to fixed n_e, T_e case: exactly the opposite of what was expected from the previous work.**

The rate coefficients have limited sensitivity to n_e, T_e over the experimental uncertainties

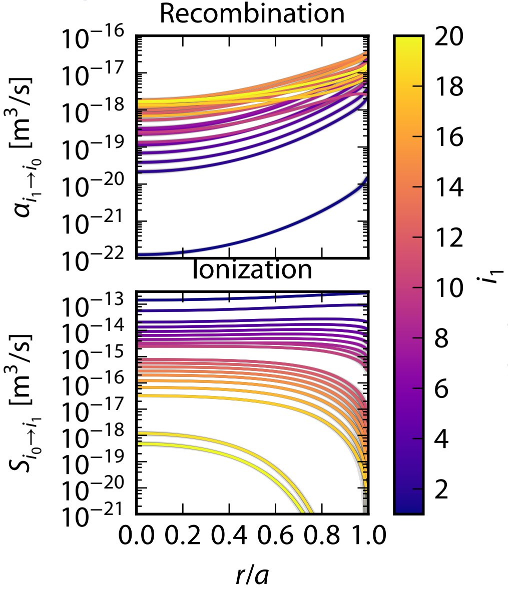

- 1000 samples from n_e, T_e
- $\pm 3\sigma$ band on α, S not even visible!
- These are the only ways that n_e, T_e enter the calculation.

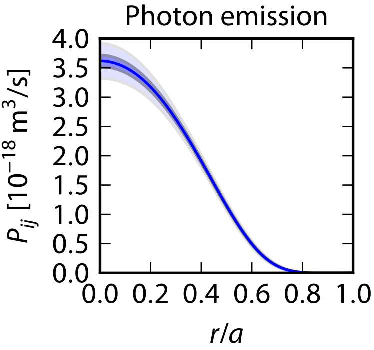

How to explain the previous result? (1)

(experimental data)

There is little correlation (ρ) between n_e, T_e and D, V

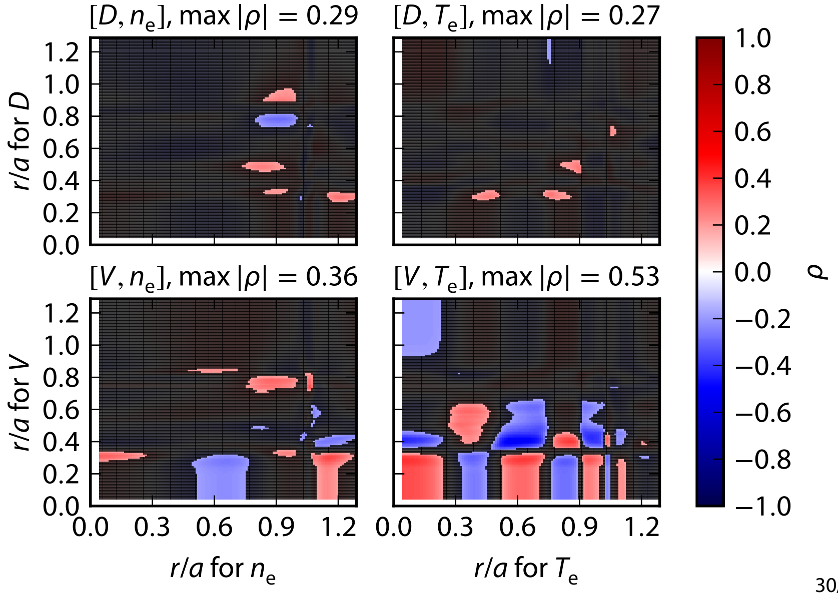

How to explain the previous result? (2)

(experimental data)

There is little correlation (ρ) between n_e, T_e and D, V

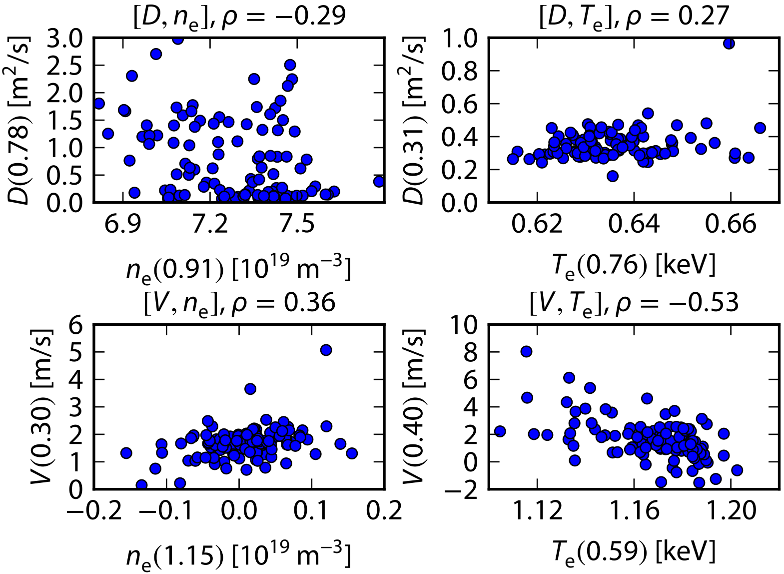

How to explain the previous result? (3)

(experimental data)

There is strong correlation (ρ) between knots and *D*, *V*

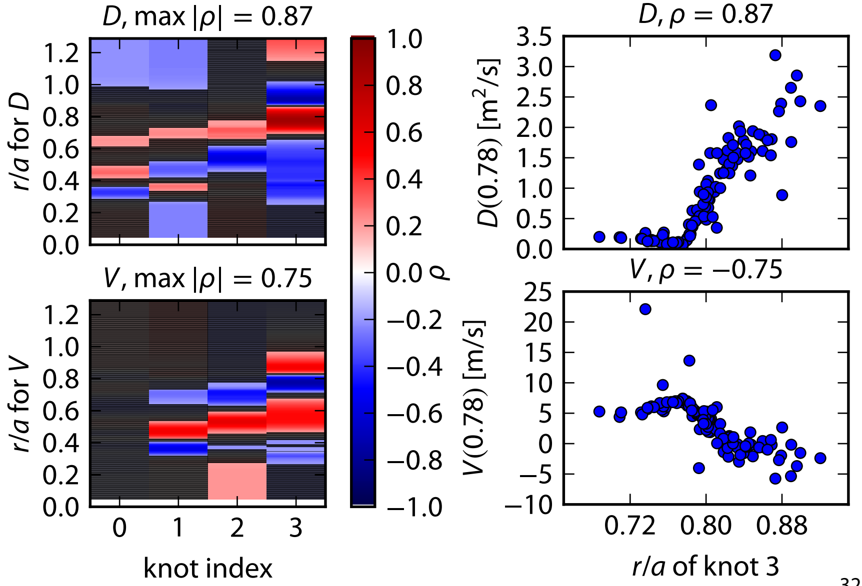

How to explain the previous result? (4)

(experimental data)

The variation seen before comes from moving the knots

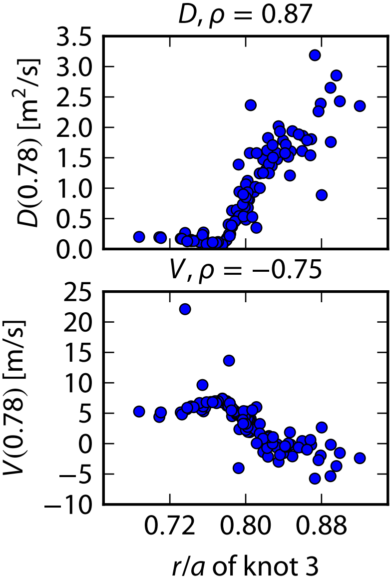

- Correlation of D, V with knot locations is *much* higher than with n_e, T_e.
- Implies the previous parameterization is too inflexible.
- Free knots cause degenerate posterior distributions, need to add *fixed position* knots.
- **Selecting the right level of complexity is critical.**

Evidence $f_y(y)$ successfully selects simple model

(synthetic data)

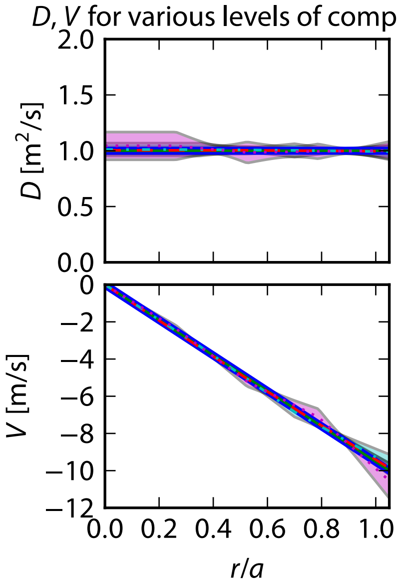

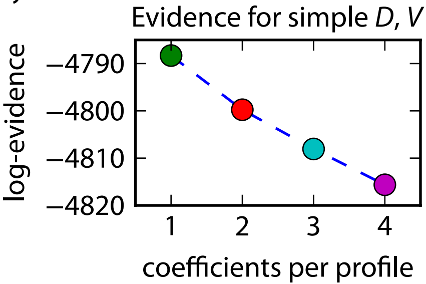

- True model has 1 coefficient.
- Linear trend is consistent with [Schwarz AS 1978]:

$$\ln f_y(y) \approx \ln f_{y|\hat{\theta}}(y|\hat{\theta}) - \frac{d}{2}\ln N$$

(d is number of parameters)

Testing with more complicated synthetic data

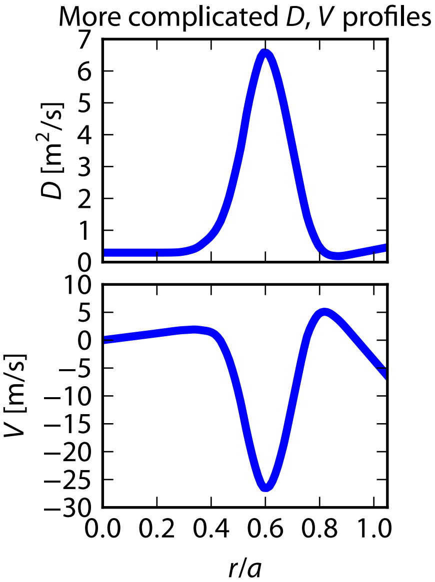

- Used result from old analysis as true profile:
  - Linear splines with 5 coefficients
  - Spline knots randomly varied to produce smooth curve
- Realistic diagnostic configuration:
  - 32 HiReX-SR chords (Ca^{18+}), 6 ms time resolution, 5% noise
  - 2 VUV chords (Ca^{17+}, Ca^{16+}), 2 ms time resolution, 5% noise

More complicated synthetic data pose a challenge

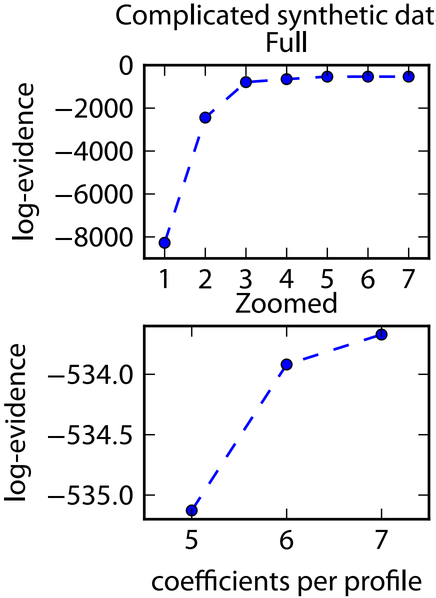

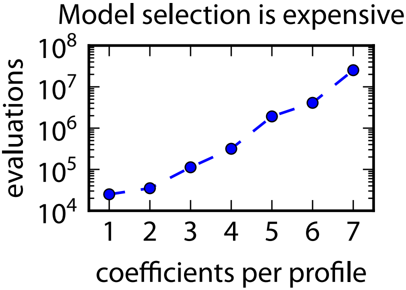

- 7 coefficient case took 7000 CPU-hours = 15 wall-clock days!
- Need to speed up STRAHL, deploy on cluster to make this practical.

Results only resemble true profile when a minimum level of complexity is obtained…despite "good" match to data

(synthetic data)

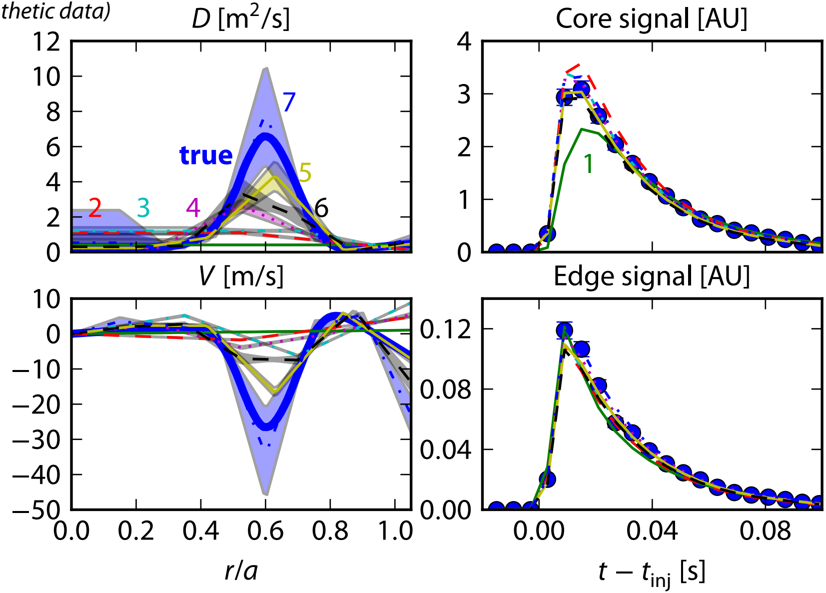

Getting *D*, *V* right is very difficult

- Do not need to worry about n_e, T_e uncertainties. ☺
- ***Need*** to select appropriate model complexity rigorously:
  - Any result obtained using overly simple functions to describe *D*, *V* is questionable.

  → **There is now an opportunity to reassess our entire picture of how well gyrokinetics describes impurity transport.** ☺
  - Proper model selection is *very* time consuming. ☹

Always ask the following:

1. How is parameter estimation performed? How are parameter uncertainties estimated?
2. How is model selection performed? Is a reasonable level of complexity for *D*, *V* used?
3. Was the analysis procedure thoroughly verified with *realistic* synthetic data?

Experimental data analysis techniques for validation of tokamak impurity transport simulations

1. Motivation: validation of turbulent transport simulations
2. Profile fitting with nonstationary Gaussian process regression
3. Inferring impurity transport coefficients: a very difficult inverse problem
4. Conclusions and future directions

Publications

Published

Chilenski NF 2015	Use of nonstationary GPR to fit L-mode profiles, propagate uncertainty.
Chilenski CPC 2016	Open source Python code for working with magnetic reconstruction data.

In progress

- Inferring *second* derivatives to test theories of momentum transport.
- Profile fitting incorporating TCI data.
- Profile fitting incorporating mtanh mean function.
- New approaches for making nonstationary Gaussian processes.
- Linearized impurity transport analysis.
- Complete impurity transport analysis.

Conclusions, contributions, and future work

Contributions of this thesis work

- New procedure and accompanying software for fitting plasma profiles: **can improve all validation efforts.**
- Linearized model for estimating diagnostic requirements: **time resolution is not as important as was previously believed.**
- Full procedure for inferring *D*, *V*: **model selection is critical,** $\boldsymbol{n_e}$**,** $\boldsymbol{T_e}$ **have minimal effect.**

Future directions to build on this work

- Streamline impurity transport analysis, deploy on cluster.
- Handle sawteeth properly.
- Reassess validation of impurity transport simulations.

"The Freidberg question" scorecard:  =8,  =1,  =3